European Journal of Mechanics / B Fluids 119 (2026) 204526

Contents lists available at ScienceDirect

European Journal of Mechanics / B Fluids

journal homepage: www.elsevier.com/locate/ejmflu

Steady channel flow of a Bingham fluid with non-flat walls: Analytical solution up to first-order perturbation terms

Lorenzo Fusi *, Angiolo Farina

Dipartimento di Matematica e Informatica "U. Dini" Università degli studi di Firenze, Viale Morgagni 67/a 50134 Firenze, Italy

ARTICLE INFO

Keywords:
Bingham fluids
Asymptotic expansion
Lubrication approximation
Yield surface dynamics
Non-Newtonian channel flow

ABSTRACT

This work investigates the steady flow of an incompressible Bingham fluid in a planar channel with non-flat walls. By exploiting a small-aspect-ratio assumption, we construct an asymptotic expansion in the geometric parameter ϵ and derive the full solution up to first order. At leading order, the analysis recovers the classical structure with a continuous rigid plug, whose velocity is determined through a nonlinear algebraic equation derived from the momentum balance in the unyielded region. The first-order problem is shown to be fully linear, with all coefficients depending solely on the zeroth-order solution. Explicit formulas for the first-order corrections to the velocity field, pressure gradient, and yield surface are obtained. Numerical tests demonstrate that these corrections are typically negligible but may reach up to 10% under specific parameter combinations. The results clarify the robustness and limitations of lubrication-type approximations for viscoplastic flows in channels of variable width.

1. Introduction

In this study, we analyze the flow of an incompressible Bingham fluid in a symmetric planar channel of non-uniform width. A Bingham fluid is a non-Newtonian fluid characterized by a yield stress threshold; for stress magnitudes below this threshold, the material behaves as a rigid solid, whereas above it, the behavior is Newtonian, [1].

The determination of the yield surface – i.e. the region where the modulus of the stress is equal to the threshold – in lubrication-type flows of viscoplastic fluids has been extensively investigated over the past decades, both within the classical Bingham framework and in more general Herschel–Bulkley models. Foundational studies on viscoplastic flow established the mathematical structure of yielded and unyielded regions in pressure-driven configurations, clarifying the role of the yield criterion in defining plug regions and free boundaries [2,3]. In thin-film and squeeze-flow settings, lubrication analyses provided explicit relations between the pressure gradient and plug thickness, enabling analytical identification of yield surfaces under long-wave scalings [4–6]. Subsequent asymptotic investigations revisited the internal structure of the pseudo-plug region and examined the consistency of lubrication approximations in viscoplastic media [7–10]. Comprehensive treatments and reviews of steady viscoplastic flows further document the analytical characterization of yielded/unyielded interfaces in confined geometries and highlight benchmark solutions that serve as reference problems for thin-layer flows [11–15].

Within this well-developed theoretical framework, the present work contributes by extending the study of lubrication approximation of a Bingham flow to the first order in closed form, thereby addressing an aspect that has not yet been systematically resolved in existing lubrication-based analyses of yield-stress fluids. Indeed, most available analytical results are restricted to flat geometries or to leading-order lubrication approximations, and systematic higher-order corrections for channels with spatially varying width remain largely unexplored. In particular, explicit first-order corrections to the velocity field, pressure gradient, and yield surface in non-uniform planar channels have not been derived in closed form. The present work addresses this gap by constructing a first order asymptotic expansion in the small-aspect-ratio parameter for the steady flow of a Bingham fluid in a planar channel with non-flat walls.

When the aspect ratio ϵ, defined as the ratio between the characteristic channel width and its length, is small, the problem can be solved analytically via an asymptotic expansion in ϵ, specifically by examining the zero-order approximation of this expansion. It is well established that this zero-order problem leads to the well-known lubrication paradox [16–19] wherein the longitudinal velocity in the unyielded domain depends on the longitudinal coordinate itself. This is an evident contradiction, since the unyielded part must behave as a rigid body and its translational velocity cannot depend on any spatial variables.

* Corresponding author.
E-mail address: lorenzo.fusi@unifi.it (L. Fusi).

https://doi.org/10.1016/j.euromechflu.2026.204526
Received 11 December 2025; Received in revised form 20 February 2026; Accepted 23 March 2026
Available online 18 April 2026
0997-7546/© 2026 The Authors. Published by Elsevier Masson SAS. This is an open access article under the CC BY license (http://creativecommons.org/licenses/by/4.0/).

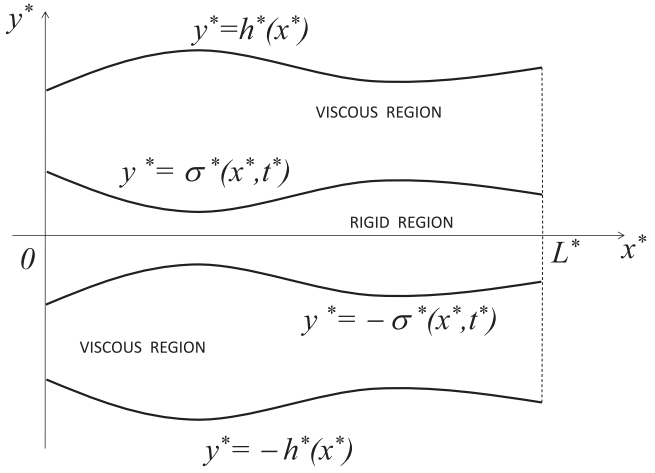


Fig. 1. Schematic depiction of the flow channel.

In [4], this paradox was circumvented by going beyond the leading-order lubrication approximation. At these higher orders, it was shown that the unyielded domain, also referred to as "plug", is not perfectly rigid: there is weak yielding (or weak deformation), i.e., the "plug" becomes a pseudo-plug. This means that, at higher order, the yield surface and the internal velocity field adjust so that mass conservation is satisfied. Another way to circumvent the lubrication paradox was proposed in [20]. In that paper, the paradox was resolved by employing an integral (rather than differential) formulation of the momentum balance equation for the rigid core. Specifically, this formulation does not require knowledge of the stress state within the unyielded region, which, being a rigid body, is indeed indeterminate. In particular, when the channel discharge (which is constant due to the mechanical incompressibility of the fluid) is prescribed, the unyielded core velocity, obtained by solving an algebraic equation, is found to be constant, consistent with rigid body behavior. In [20] and in subsequent works [18,21,22], the analysis of the solution was confined to the zero order, under the fundamental assumption that the rigid core extends continuously, i.e., without interruptions, along the entire channel.

In this paper, we extend the asymptotic analysis to first order in ε, in order to evaluate the significance of the $\mathcal{O}(\varepsilon)$ correction terms in the asymptotic expansion. In Section 2, we formulate the governing balance equations and the boundary conditions and render them dimensionless. Next, in Section 3 we look for the solution in the form of an asymptotic series, restricting our analysis to the $\mathcal{O}(\varepsilon^0)$ and $\mathcal{O}(\varepsilon)$ terms. In Section 4 we show that, in accordance with the findings of [21], all the zero-order primary variables are determined as functions of the uniform value of the unyielded inner core velocity, which is found by solving a nonlinear algebraic equation derived from the rigid region momentum balance. The $\mathcal{O}(\varepsilon)$ problem is analyzed in Section 5. This problem is solved by expressing all first-order unknowns in terms of the first-order correction to the rigid core velocity, which itself is a function of the zero-order core velocity. Consequently, the expressions for the first-order corrections (as indeed all problems of order larger than zero) are explicitly written in terms of the zero-order solution. Section 6 is devoted to the results of the numerical simulations and to their interpretation. In particular, it is shown that the first-order corrections are almost always negligible (if ε is sufficiently small), except in certain cases (which occur for specific choices of the dimensionless parameters) in which they can reach up to 10% of the values obtained at zero order. Finally, the last section summarizes the main results and discusses their relevance to the dynamics of Bingham fluids.

2. Derivation of the model

We consider the stationary flow of an incompressible Bingham fluid in a symmetric channel of length[1] L^* and width $2h^*(x^*)$, as depicted in . The velocity field is given by

$$\mathbf{v}^* = u^*(x^*, y^*)\mathbf{i} + v^*(x^*, y^*)\mathbf{j},$$

where x^* and y^* are the longitudinal and transverse coordinates, respectively. We further assume that the viscous and rigid parts of the flow are separated by a sharp interface $y^* = \pm\sigma^*(x^*, t^*)$, which extends seamlessly from the inlet, $x^* = 0$, to the outlet, $x^* = L^*$. Due to symmetry, we confine our analysis to the upper part of the channel, i.e., $y^* \in [0, h^*]$.

The Cauchy stress is written as $\mathbf{T}^* = -p^*\mathbf{I} + \mathbf{S}^*$, where $p^* = 1/3\,\mathrm{tr}\,\mathbf{T}^*$ represents the pressure and $\mathbf{S}^*$ is the extra-stress. We assume that whenever the invariant

$$II_{S^*} = \sqrt{\frac{1}{2}\mathbf{S}^* \cdot \mathbf{S}^*} \geqslant \tau_o^*,$$

the tensor $\mathbf{S}^*$ is given by

$$\mathbf{S}^* = \left(2\mu^* + \frac{\tau_o^*}{II_{D^*}}\right)\mathbf{D}^*, \tag{1}$$

where μ^* is the viscosity, τ_o^* is the stress threshold, and

$$\mathbf{D}^* = \frac{1}{2}\left(\nabla\mathbf{v}^* + \nabla\mathbf{v}^{*\,\mathrm{T}}\right), \qquad II_{D^*} = \sqrt{\frac{1}{2}\mathbf{D}^* \cdot \mathbf{D}^*},$$

are the symmetric part of the velocity gradient and its corresponding invariant, respectively. When $II_{S^*} < \tau_o^*$, the material behaves as a rigid body with $\mathbf{D}^* = 0$. Hence, at the yield surface, we have

$$II_{D^*}\big|_{\sigma^*} = 0. \tag{2}$$

Mechanical incompressibility implies $\mathrm{tr}\,\mathbf{D}^* = 0$, namely

$$\frac{\partial u^*}{\partial x^*} + \frac{\partial v^*}{\partial y^*} = 0. \tag{3}$$

The momentum equations for the viscous part ($II_{S^*} \geqslant \tau_o^*$), in the absence of body forces and under stationary conditions, are

$$\varrho^*\left(u^*\frac{\partial u^*}{\partial x^*} + v^*\frac{\partial u^*}{\partial y^*}\right) = -\frac{\partial p^*}{\partial x^*} + \frac{\partial S_{11}^*}{\partial x^*} + \frac{\partial S_{12}^*}{\partial y^*}, \tag{4}$$

$$\varrho^*\left(u^*\frac{\partial v^*}{\partial x^*} + v^*\frac{\partial v^*}{\partial y^*}\right) = -\frac{\partial p^*}{\partial y^*} + \frac{\partial S_{12}^*}{\partial x^*} + \frac{\partial S_{22}^*}{\partial y^*}, \tag{5}$$

where ϱ^* is the fluid density (assumed constant in both the rigid and viscous domains) and S_{ij}^* are the components of $\mathbf{S}^*$, given by (1).

We note that the half-discharge

$$Q^* = \int_0^{h^*(x^*)} u^* dy^*, \tag{6}$$

is constant due to incompressibility. In what follows, the total discharge, i.e., $2Q^*$, is a prescribed positive quantity.

The dynamics of the "plug" is governed by the balance of the forces acting on it, since we are in steady-state conditions. Following [20], we therefore obtain the following integral equation

$$0 = \int_0^{L^*} \left[-\sigma_x^* T_{11}^* + T_{12}^*\right]_{\sigma^*} dx^* + p_{in}^*\sigma_{in}^* - p_{out}^*\sigma_{out}^*, \tag{7}$$

where p_{in}^* and p_{out}^* are the applied pressures at the channel inlet and outlet, respectively, $\sigma_{in}^* = \sigma^*(0, t^*)$, $\sigma_{out}^* = \sigma^*(L^*, t^*)$ and the term $\left[-\sigma_x^* T_{11}^* + T_{12}^*\right]_{\sigma^*}$ is the force exerted by the viscous region on the lateral side of the inner rigid core.

Concerning boundary conditions, on $y^* = h^*$ we impose

$$\mathbf{v}^*(x^*, h^*) = 0, \tag{8}$$

[1] Here and in the sequel, the superscript * denotes dimensional quantities.

while on the yield surface $y^* = \sigma^*$, we impose[2]

$$[\![\mathbf{v}^* \cdot \mathbf{t}]\!]_{y^*=\sigma^*} = 0, \qquad [\![\mathbf{v}^* \cdot \mathbf{n}]\!]_{y^*=\sigma^*} = 0, \tag{9}$$

$$[\![\mathbf{T}^* \mathbf{n} \cdot \mathbf{t}]\!]_{y^*=\sigma^*} = 0, \qquad [\![\mathbf{T}^* \mathbf{n} \cdot \mathbf{n}]\!]_{y^*=\sigma^*} = 0, \tag{10}$$

which express the continuity of velocity and stress across the yield surface $y^* = \sigma^*$ (here $\mathbf{t}$ and $\mathbf{n}$ are the unit tangent and normal vectors to $y^* = \sigma^*$, respectively). Since

$$\mathbf{t} = \frac{1}{\sqrt{1 + \left(\frac{\partial \sigma^*}{\partial x^*}\right)^2}} \left(\mathbf{i} + \frac{\partial \sigma^*}{\partial x^*}\mathbf{j}\right), \qquad \mathbf{n} = \frac{1}{\sqrt{1 + \left(\frac{\partial \sigma^*}{\partial x^*}\right)^2}} \left(-\frac{\partial \sigma^*}{\partial x^*}\mathbf{i} + \mathbf{j}\right),$$

condition (9) implies

$$\begin{pmatrix} 1 & \frac{\partial \sigma^*}{\partial x^*} \\ -\frac{\partial \sigma^*}{\partial x^*} & 1 \end{pmatrix} \begin{pmatrix} [\![u^*]\!] \\ [\![v^*]\!] \end{pmatrix} = 0 \quad \Rightarrow \quad [\![u^*]\!] = [\![v^*]\!] = 0. \tag{11}$$

As stated in the introduction, we assume that the characteristic channel length L^* is much larger than its maximum half-width H^*, where $H^* = \max_{x^* \in [0, L^*]} h^*(x^*)$. We thus introduce the parameter

$$\varepsilon = \frac{H^*}{L^*} \ll 1,$$

which is crucial for applying the classical thin film approximation (or lubrication approximation).

We rescale the main quantities of the problem by taking $U^* = Q^*/H^*$ as the characteristic longitudinal velocity and introducing the following dimensionless variables

$$x = \frac{x^*}{L^*}, \qquad y = \frac{y^*}{\varepsilon L^*}, \qquad \sigma = \frac{\sigma^*}{\varepsilon L^*},$$

$$u = \frac{u^*}{U^*}, \qquad v = \frac{v^*}{\varepsilon U^*}, \qquad p = \frac{p^*}{(\mu^* U^* L^*/H^{*2})},$$

$$\mathbf{S} = \frac{\mathbf{S}^*}{(\mu^* U^*/H^*)}, \quad \mathbf{D} = \frac{\mathbf{D}^*}{(U^*/H^*)}, \quad II_D = \frac{II_{D^*}}{(U^*/H^*)}, \quad II_S = \frac{II_{S^*}}{(\mu^* U^*/H^*)}.$$

We note that the pressure has been rescaled using the Poiseuille formula, while the stress has been rescaled using the characteristic viscous stress. After some algebra, we find

$$\mathbf{D} = \begin{bmatrix} \varepsilon u_x & \frac{1}{2}\left(u_y + \varepsilon^2 v_x\right) \\ \frac{1}{2}\left(u_y + \varepsilon^2 v_x\right) & \varepsilon v_y \end{bmatrix},$$

$$\mathbf{S} = \left(2 + \frac{\mathrm{Bi}}{II_D}\right) \begin{bmatrix} \varepsilon u_x & \frac{1}{2}\left(u_y + \varepsilon^2 v_x\right) \\ \frac{1}{2}\left(u_y + \varepsilon^2 v_x\right) & \varepsilon v_y \end{bmatrix},$$

where

$$\mathrm{Bi} = \frac{\tau_o^* H^*}{\mu^* U^*},$$

is the Bingham number. Moreover,

$$II_D = \sqrt{\varepsilon^2 u_x^2 + \frac{1}{4}\left(u_y + \varepsilon^2 v_x\right)^2}, \tag{12}$$

and (2) becomes

$$II_D\big|_\sigma = \sqrt{\varepsilon^2 u_x^2(x, \sigma, t) + \frac{1}{4}\left[u_y(x, \sigma, t) + \varepsilon^2 v_x(x, \sigma, t)\right]^2} = 0. \tag{13}$$

The dimensionless form of problem (3)–(5) is

$$u_x + v_y = 0, \tag{14}$$

$$\varepsilon \mathrm{Re}\left(u u_x + v u_y\right) = -p_x + \varepsilon S_{11\ x} + S_{12\ y}, \tag{15}$$

$$\varepsilon^3 \mathrm{Re}\left(u v_x + v v_y\right) = -p_y + \varepsilon^2 S_{12\ x} + \varepsilon S_{22\ y}, \tag{16}$$

where

$$\mathrm{Re} = \frac{\rho^* U^* H^*}{\mu^*},$$

is the Reynolds number.

At this stage, we explicitly state the formal validity conditions of the asymptotic expansion: $\varepsilon \ll 1$ and $\mathrm{Re} = O(1)$, so that inertial effects enter only as first-order corrections in (15).

Condition (6) becomes

$$\int_0^h u \, dy = 1, \tag{17}$$

and Eq. (7) becomes

$$0 = \int_0^1 \left[-p_x \sigma - \varepsilon \sigma_x S_{11} + S_{12}\right]_\sigma \, dx. \tag{18}$$

The boundary conditions (8), (11), and (10) become

$$\mathbf{v}(x, h(x)) = 0, \tag{19}$$

$$[\![u(x, \sigma)]\!] = 0, \qquad [\![v(x, \sigma)]\!] = 0, \tag{20}$$

$$\begin{cases} [\![-p\left(1 + \varepsilon_x^2 \sigma^2\right)]\!] + [\![\varepsilon^3 S_{11} \sigma_x^2 - 2\varepsilon^2 S_{12} \sigma_x + \varepsilon S_{22}]\!] = 0, \\ [\![\varepsilon \sigma_x \left(S_{22} - S_{11}\right) + S_{12}\left(1 - \varepsilon^2 \sigma_x\right)]\!] = 0. \end{cases} \tag{21}$$

The dimensionless longitudinal velocity of the inner rigid core cannot depend on x, and its transverse velocity must vanish. Therefore, conditions (20) imply

$$\frac{d}{dx}\left[u(x, \sigma(x))\right] = 0, \quad \text{and} \quad v(x, \sigma) = 0. \tag{22}$$

Remark 1. We observe that the Reynolds number Re and the Bingham number Bi are not independent, since both depend on the characteristic velocity U^*. In particular, it can be easily verified that

$$\mathrm{Re} = \frac{\Gamma}{\mathrm{Bi}}, \qquad \Gamma = \left(\frac{\rho^* \tau_o^* H^{*2}}{\mu^{*2}}\right), \tag{23}$$

where Γ is a non-dimensional material parameter that depends on the channel geometry and on the fluid's material properties, but not on the kinematic state, i.e., on U^*. Therefore, once the channel is specified and the fluid is selected (and thus characterized by given density, viscosity, and yield stress), the parameter Γ is fixed. Consequently, the Reynolds and Bingham numbers can vary only through changes in the kinematic state, that is, through variations in the characteristic velocity U^*, which, in our case, can occur solely by adjusting the volumetric flow rate.

3. Asymptotic expansion

We look for a solution in which the main variables of the problem can be expressed as power series in ε, namely

$$\mathbf{v} = \mathbf{v}^{(0)} + \varepsilon \mathbf{v}^{(1)} + \cdots,$$

$$p = p^{(0)} + \varepsilon p^{(1)} + \cdots,$$

$$\sigma = \sigma^{(0)} + \varepsilon \sigma^{(1)} + \cdots,$$

$$\mathbf{S} = \mathbf{S}^{(0)} + \varepsilon \mathbf{S}^{(1)} + \cdots.$$

[2] The symbol $[\![\ldots]\!]_{y^*=\sigma^*}$ denotes the jump across the interface $y^* = \sigma^*$. We also assume $[\![\rho^*]\!]_{y^*=\sigma^*} = 0$.

We now rewrite the conservation equations, constitutive equations, and boundary conditions up to first order in the perturbation parameter. Starting from (14)–(16), we obtain the governing equations at zero order

$$\begin{cases} u_x^{(0)} + v_y^{(0)} = 0, \\ -p_x^{(0)} + S_{12\ y}^{(0)} = 0, \\ -p_y^{(0)} = 0, \end{cases} \tag{24}$$

and first order

$$\begin{cases} u_x^{(1)} + v_y^{(1)} = 0, \\ \mathsf{Re}\left(u^{(0)} u_x^{(0)} + v^{(0)} u_y^{(0)}\right) = -p_x^{(1)} + S_{11\ x}^{(0)} + S_{12\ y}^{(1)}, \\ -p_y^{(1)} + S_{22\ y}^{(0)} = 0. \end{cases} \tag{25}$$

Concerning (17), we have

$$\begin{cases} \int_0^h u^{(0)} dy = 1, \\ \int_0^h u^{(1)} dy = 0. \end{cases} \tag{26}$$

Next, we enforce (19), (13), and (22). At zero order we obtain

$$u^{(0)}(x,h) = v^{(0)}(x,h) = 0, \tag{27}$$

and

$$\begin{cases} u_y^{(0)}\left(x,\sigma^{(0)}\right) = 0, \\ \frac{d}{dx}\left[u^{(0)}\left(x,\sigma^{(0)}\right)\right] = 0, \\ v^{(0)}\left(x,\sigma^{(0)}\right) = 0. \end{cases} \tag{28}$$

We remark that $(28)_1$, $(28)_{2,\text{motion-01}}$ imply

$$u_x^{(0)}\left(x,\sigma^{(0)}\right) = -v_y^{(0)}\left(x,\sigma^{(0)}\right) = 0. \tag{29}$$

At first order, we have

$$u^{(1)}(x,h) = v^{(1)}(x,h) = 0, \tag{30}$$

and

$$\begin{cases} u_{yy}^{(0)}\left(x,\sigma^{(0)}\right)\sigma^{(1)} + u_y^{(1)}\left(x,\sigma^{(0)}\right) = 0, \\ \frac{d}{dx}\left[u_y^{(0)}\left(x,\sigma^{(0)}\right) + u^{(1)}\left(x,\sigma^{(0)}\right)\right] = 0, \\ v_y^{(0)}\left(x,\sigma^{(0)}\right) + v^{(1)}\left(x,\sigma^{(0)}\right) = 0, \end{cases}$$

which, because of (29), reduces to

$$\begin{cases} u_{yy}^{(0)}\left(x,\sigma^{(0)}\right)\sigma^{(1)} + u_y^{(1)}\left(x,\sigma^{(0)}\right) = 0, \\ \frac{d}{dx}\left[u^{(1)}\left(x,\sigma^{(0)}\right)\right] = 0, \\ v^{(1)}\left(x,\sigma^{(0)}\right) = 0. \end{cases} \tag{31}$$

We now provide the structure of the components of $\mathbf{S}$ at zero and at first order. We have

$$\begin{cases} S_{11}^{(0)} = 0, \\ S_{22}^{(0)} = 0, \\ S_{12}^{(0)} = u_y^{(0)} - \mathsf{Bi}, \end{cases} \tag{32}$$

at zero order, and

$$\begin{cases} S_{11}^{(1)} = \dfrac{2\left(u_y^{(0)} - \mathsf{Bi}\right)u_x^{(0)}}{u_y^{(0)}}, \\ S_{22}^{(1)} = -\dfrac{2\left(u_y^{(0)} - \mathsf{Bi}\right)u_x^{(0)}}{u_y^{(0)}}, \\ S_{12}^{(1)} = u_y^{(1)}, \end{cases} \tag{33}$$

at first order. Finally, by focusing on the rigid core Eq. (18), we obtain

$$\int_0^1 \left(p_x^{(0)}(x)\,\sigma^{(0)} + \mathsf{Bi}\right) dx = 0, \tag{34}$$

at the zero order, and

$$\int_0^1 \left[p_x^{(0)}(x)\,\sigma^{(1)} + p_x^{(1)}\left(x,\sigma^{(0)}\right)\sigma^{(0)}\right] dx = 0, \tag{35}$$

at first order.

4. Zero order

Using (24), (32), and (27), we find that $p^{(0)} = p^{(0)}(x)$ and

$$u^{(0)}(x,y) = \begin{cases} -\dfrac{p_x^{(0)}(x)}{2}\left[\left(h-\sigma^{(0)}\right)^2 - \left(y-\sigma^{(0)}\right)^2\right], & y \in \left[\sigma^{(0)}, h\right], \\ -\dfrac{p_x^{(0)}(x)}{2}\left(h-\sigma^{(0)}\right)^2, & y \in \left[0, \sigma^{(0)}\right]. \end{cases} \tag{36}$$

In particular, we define

$$u_c^{(0)} = -\frac{p_x^{(0)}(x)}{2}\left[h(x) - \sigma^{(0)}(x)\right]^2, \tag{37}$$

which, due to $(28)_2$, is uniform with respect to x, i.e.,

$$\frac{du_c^{(0)}}{dx} = 0.$$

The transverse velocity is obtained using $(24)_1$, (27), and $(28)_3$

$$v^{(0)}(x,y) = \begin{cases} \dfrac{2{u_c^{(0)}}^2 h_x (h-y)\left(2u_c^{(0)}h + u_c^{(0)}y - 3\right)^2}{27\left(u_c^{(0)}h - 1\right)^3}, & y \in \left[\sigma^{(0)}, h\right], \\ 0, & y \in \left[0, \sigma^{(0)}\right]. \end{cases}$$

Enforcing $(26)_1$ and using (37), we obtain

$$\begin{cases} \sigma^{(0)}(x) = \dfrac{3}{u_c^{(0)}} - 2h(x), \\ p_x^{(0)}(x) = -\dfrac{2\left(u_c^{(0)}\right)^3}{9\left(h(x)\,u_c^{(0)} - 1\right)^2}. \end{cases} \tag{38}$$

To close the problem, it is therefore necessary to determine $u_c^{(0)}$, since all the dependent variables, namely $u^{(0)}(x,y)$, $v^{(0)}(x,y)$, $\sigma^{(0)}(x)$ and $p_x^{(0)}(x)$, are expressed as functions of the profile $h(x)$ and of $u_c^{(0)}$. The latter is found using (34), which yields the following algebraic equation in the unknown $u_c^{(0)}$

$$\mathcal{F}(u_c^{(0)}) = \mathsf{Bi}, \tag{39}$$

where

$$\mathcal{F}(u_c^{(0)}) = \int_0^1 \frac{2\left(u_c^{(0)}\right)^2\left(3 - 2h(x)\,u_c^{(0)}\right)}{9\left(h(x)\,u_c^{(0)} - 1\right)^2} dx. \tag{40}$$

In particular, setting $h_{min} = \min_{x\in[0,1]} h(x)$, it can be proved (see, e.g., [21]) that $\mathcal{F}(\xi)$ is a continuous, monotonically decreasing function over the domain $(1/h_{min}, 3/2]$ (where we assume that $2/3 < h_{min}$) and $\lim_{\xi\to 1/h_{min}} \mathcal{F}(\xi) = +\infty$. As an immediate consequence, Eq. (39) admits a unique solution $u_c^{(0)}$ in the interval $(1/h_{min}, 3/2]$ if and only if

$$\mathsf{Bi} \in \left[\mathcal{F}(3/2),\ \infty\right). \tag{41}$$

Based on the existence and uniqueness of the solution of (39), provided (41) and $2/3 < h_{min}$ hold true, it follows that all subsequent problems at higher orders of approximation are well posed, as they are linear in nature.

In particular, exploiting (38), the longitudinal velocity component $u^{(0)}(x,y)$ can also be written, in the viscous region, in terms of $u_c^{(0)}$, $h(x)$ and the y variable, namely

$$u^{(0)}(x,y) = \frac{u_c^{(0)^2}(h(x)-y)\left(5h(x)u_c^{(0)} + yu_c^{(0)} - 6\right)}{9(h(x)u_c^{(0)}-1)^2}, \qquad (x,y)\in[0,1]\times[\sigma^{(0)},h].$$

Finally, we note that when h is expressed in polynomial form, Eq. (39) can, in general, be integrated analytically, yielding a purely algebraic nonlinear expression in $u_c^{(0)}$. In the case $h(x) = 1$, this equation reduces to the so-called Buckingham equation, see [1].

5. First order

We begin with (25), which, using (32), yields

$$\begin{cases} u_x^{(1)} + v_y^{(1)} = 0, \\ -p_x^{(1)} + S_{12\ y}^{(1)} = \mathsf{Re}\left(u^{(0)}u_x^{(0)} + v^{(0)}u_y^{(0)}\right), \qquad \Longrightarrow \qquad p^{(1)} = p^{(1)}(x). \\ p_y^{(1)} = 0, \end{cases}$$

Using $(33)_3$, we can write the following equation for $u^{(1)}$

$$u_{yy}^{(1)} = p_x^{(1)}(x) + \mathsf{Re}\left(u^{(0)}u_x^{(0)} + v^{(0)}u_y^{(0)}\right), \tag{42}$$

which we integrate using boundary conditions $(31)_{1,\text{bc-h-1}}$ and thus obtain

$$u^{(1)}(x,y) = u_{yy}^{(0)}\left(x,\sigma^{(0)}\right)\sigma^{(1)}(h-y) - \frac{p_x^{(1)}(x)}{2}\left[\left(h-\sigma^{(0)}\right)^2 - \left(y-\sigma^{(0)}\right)^2\right] - \mathsf{Re}\int_y^h dy'\int_{\sigma^{(0)}}^{y'}\left(u^{(0)}u_x^{(0)} + v^{(0)}u_y^{(0)}\right)dy''.$$

Introducing the definition

$$u_c^{(1)} = u^{(1)}\left(x,\sigma^0\right),$$

which, because of $(31)_2$, is uniform with respect to x, we have

$$u_c^{(1)} = u_{yy}^{(0)}\left(x,\sigma^{(0)}\right)\sigma^{(1)}\left(h-\sigma^{(0)}\right) - \frac{p_x^{(1)}(x)}{2}\left(h-\sigma^{(0)}\right)^2 - \mathsf{Re}\int_{\sigma^{(0)}}^h dy'\int_{\sigma^{(0)}}^{y'}\left(u^{(0)}u_x^{(0)} + v^{(0)}u_y^{(0)}\right)dy''. \tag{43}$$

We therefore can rewrite $u^{(1)}$ as the equation given in Box I.

with $u_c^{(1)}$ given by (43). We now enforce (26), which at first order takes the form

$$\int_{\sigma^{(0)}}^h u^{(1)}(x,y)\,dy + u_c^{(1)}\sigma^{(0)} = 0,$$

namely,

$$u_c^{(1)}h - u_{yy}^{(0)}\left(x,\sigma^{(0)}\right)\sigma^{(1)}\frac{\left(h-\sigma^{(0)}\right)^2}{2} + \frac{p_x^{(1)}(x)}{6}\left(h-\sigma^{(0)}\right)^3 + \mathsf{Re}\int_{\sigma^{(0)}}^h dy\int_{\sigma^{(0)}}^{y} dy'\int_{\sigma^{(0)}}^{y'}\left(u^{(0)}u_x^{(0)} + v^{(0)}u_y^{(0)}\right)dy'' = 0.$$

By using (43) to express the term $\frac{p_x^{(1)}(x)}{2}\left(h-\sigma^{(0)}\right)^2$ in the previous expression, we obtain the following linear equation in $\sigma^{(1)}(x)$

$$\begin{aligned} &u_c^{(1)}h - \sigma^{(1)}u_{yy}^{(0)}\left(x,\sigma^{(0)}\right)\frac{\left(h-\sigma^{(0)}\right)^2}{2} \\ &+\frac{\left(h-\sigma^{(0)}\right)}{3}\left[-u_c^{(1)} + \sigma^{(1)}u_{yy}^{(0)}\left(x,\sigma^{(0)}\right)\frac{\left(h-\sigma^{(0)}\right)^2}{2}\right. \\ &\left.-\mathsf{Re}\int_{\sigma^{(0)}}^h dy'\int_{\sigma^{(0)}}^{y'}\left(u^{(0)}u_x^{(0)} + v^{(0)}u_y^{(0)}\right)dy''\right] \\ &+\mathsf{Re}\int_{\sigma^{(0)}}^h dy\int_{\sigma^{(0)}}^{y} dy'\int_{\sigma^{(0)}}^{y'}\left(u^{(0)}u_x^{(0)} + v^{(0)}u_y^{(0)}\right)dy'' = 0. \end{aligned} \tag{44}$$

Thus, by solving (44), we obtain an expression for $\sigma^{(1)}(x)$ in terms of $u_c^{(1)}$, $h(x)$, and the zeroth-order quantities $u^{(0)}$ and $v^{(0)}$. We then use (43) to derive an expression for $p_x^{(1)}$ in terms of $u_c^{(1)}$, $h(x)$, and the zeroth-order quantities as well. The final step is to use Eq. (35) to derive a linear equation for $u_c^{(1)}$. At the end of this procedure, which is algebraically very lengthy but conceptually very simple, we obtain

$$\sigma^{(1)}(x) = \left[-\frac{3}{u_c^{(0)}}\right]u_c^{(1)} - \frac{3\mathsf{Re}\left(h(x)u_c^{(0)}-1\right)^2 h_x(x)}{70u_c^{(0)}}, \tag{45}$$

$$p_x^{(1)}(x) = \left[-\frac{2u_c^{(0)^2}\left(h(x)u_c^{(0)}-3\right)}{9\left(h(x)u_c^{(0)}-1\right)^2}\right]u_c^{(1)} + \frac{17\mathsf{Re}u_c^{(0)^3}h_x(x)}{105\left(h(x)u_c^{(0)}-1\right)}, \tag{46}$$

$$u_c^{(1)} = \left(\frac{u_c^{(0)^2}\mathsf{Re}}{105}\right)\frac{\int_0^1 \frac{h_x(x)\left(33h(x)u_c^{(0)}-50\right]}{\left(h(x)u_c^{(0)}-1\right)}dx}{\int_0^1 \frac{4\left[h^2(x)u_c^{(0)^2} - 3h(x)u_c^{(0)} + 3\right]u_c^{(0)}}{9\left(h(x)u_c^{(0)}-1\right)^3}dx}. \tag{47}$$

So, once we have obtained $u_c^{(1)}$ from (47), we substitute it into the expressions for the yield surface $\sigma^{(1)}$(45), for the pressure gradient $p_x^{(1)}$(46), for the longitudinal velocity $u^{(1)}$ (48) and for the transverse velocity $v^{(1)}$ (whose expression is too lengthy to be reported here). In this way, we have determined all the main first-order variables in terms of quantities that depend exclusively on the zeroth-order solution.

Before concluding the section, we would like to draw the readers' attention to a couple of points that we believe are noteworthy. The first is that the first-order corrections vanish when the flow takes place in a channel whose walls are flat. In fact, if $h = 1$, then $h_x = 0$ and consequently $u_c^{(1)} = 0$, and all other first-order quantities vanish. In this case, the problem is fully determined at zero order, and Eq. (39) reduces to the well-known Buckingham equation [1]. The second fact that has emerged from the analysis so far is that, to first order, all dependent variables are determined by linear problems, or linear algebraic equations, in which the coefficients and known terms are functions of the zeroth-order variables. This structure, although not explicitly proven at this step, is preserved for higher orders as well. Consequently, the corrections at order $n+1$ are determined by linear problems or algebraic equations. Since at zeroth order the coefficients remain uniformly bounded with respect to ε, the corrections at any order n will also be bounded. It follows that the nth remainder of the asymptotic series remains bounded with respect to ε, and hence the expansion is well posed. Certainly this does not prove the convergence of the series in a rigorous way, but it clearly tells us that the solution remains bounded at any order.

$$u^{(1)}(x,y)=\begin{cases} u_c^{(1)}+u_{yy}^{(0)}\left(x,\sigma^{(0)}\right)\sigma^{(1)}\left(\sigma^{(0)}-y\right)+\dfrac{p_x^{(1)}(x)}{2}\left(y-\sigma^{(0)}\right)^2 & \\ +\mathsf{Re}\displaystyle\int_{\sigma^{(0)}}^{y}dy'\int_{\sigma^{(0)}}^{y'}\left(u^{(0)}u_x^{(0)}+v^{(0)}u_y^{(0)}\right)dy'', & (x,y)\in[0,1]\times\left[\sigma^{(0)}(x),h(x)\right], \\ u_c^{(1)}, & (x,y)\in[0,1]\times\left[0,\sigma^{(0)}(x)\right], \end{cases} \tag{48}$$

Box I.

6. Results and discussion

In this section, we consider several channel profiles to analyze the contribution of the first-order correction. We begin by considering a converging channel with wall profile

$$\begin{cases} h(x)=a\,\mathrm{erf}\left[b\left(\dfrac{1}{2}-x\right)\right]+c, \\ a=\dfrac{3}{20\,\mathrm{erf}\left(\dfrac{b}{2}\right)}, \qquad b=20, \qquad c=\dfrac{17}{20}, \end{cases} \tag{49}$$

as shown in Fig. 2(a). The choice of (49) is compatible with the condition $h_{min}>3/2$, which ensures, for Bi satisfying (41), that the rigid plug extends along the entire length of the channel without interruptions.

Assuming $\varepsilon=10^{-2}$ and $\Gamma=100$, we observe that Bi must be selected so as to satisfy $\mathsf{Bi}>\mathcal{F}(3/2)\approx 79.22$. We note that when $\mathsf{Bi}=\mathcal{F}(3/2)$, the value of the Reynolds number obtained via (23) is 1.26, so that $\varepsilon\mathsf{Re}\approx 10^{-2}$, which provides an "a posteriori check" that the inertial part of the momentum Eqs. (15)–(16) can be safely neglected. Any value of Bi larger than 79.22 is then admissible, since it will produce a lower Re and hence smaller inertial effects.

The order of magnitude of the first-order correction to the yield surface is $\max_{[0,1]}(|\varepsilon\sigma^{(1)}|=1.43\cdot 10^{-4})$. This implies that, in Fig. 2(a), $\sigma^{(0)}$ is practically indistinguishable from $\sigma^{(0)}+\varepsilon\sigma^{(1)}$. However, since we are considering dimensionless variables, we are more interested in the relative error than in the absolute one. Therefore, we consider the quantity

$$\mathcal{E}(x)=\left|1-\frac{\varepsilon\sigma^{(1)}(x)}{\sigma^{(0)}(x)}\right|\cdot 100, \tag{50}$$

which represents the percentage relative error. The function $\mathcal{E}(x)$ is always well defined, since $\sigma^{(0)}>0$ for $x\in[0,1]$. The plot of the relative error is shown in Fig. 2(b) for various Bi satisfying (41), with the material parameter Γ defined in (23). We see that the relative error decreases as Bi increases.

The example presented above uses model parameters (such as the Bingham number, Reynolds number, and so on) that are consistent with the asymptotic analysis, but are otherwise arbitrary and not associated with any specific, real viscoplastic fluids. To demonstrate the practical relevance of the proposed approximation, we now consider parameter values corresponding to actual viscoplastic fluids, providing the bibliographic references from which these values are taken. In all these examples, the wall profile $h(x)$ is the non-monotonic function

$$h(x)=\frac{9}{10}+\frac{1}{10}\sin\left(2\pi x\right), \tag{51}$$

with $h_{min}=0.8>2/3$ and $\mathcal{F}(3/2)=2.37$. Therefore, the admissible Bingham numbers are those satisfying $\mathsf{Bi}>2.37$. For each fluid considered, we must verify that the product $\varepsilon\mathsf{Re}$ is sufficiently small (e.g. $\leqslant\mathcal{O}(10^{-1})$).

As a first real-world example, we consider the so-called "drilling muds" reported in [23]. Table 1 lists typical values of the material, geometric, and flow parameters associated with this class of viscoplastic fluids. The corresponding non-dimensional numbers Re, Bi, and Γ are also provided.

Table 1
Drilling mud parameters, from [23].

ρ^*	τ_o^*	μ^*	H^*	U^*	Bi	Re	Γ	ε
1040 $\frac{\mathrm{kg}}{\mathrm{m}^3}$	2.5 Pa	0.2 Pa s	0.01 m	0.1 m/s	2.5	10.4	26	10^{-2}

Table 2
Toothpaste parameters, from [24].

ρ^*	τ_o^*	μ^*	H^*	U^*	Bi	Re	Γ	ε
1400 $\frac{\mathrm{kg}}{\mathrm{m}^3}$	250 Pa	40 Pa s	0.05 m	0.1 m/s	3.12	0.17	0.54	0.5

Fig. 3(a) displays the yield surfaces $\sigma^{(0)}$ and $\sigma^{(0)}+\varepsilon\sigma^{(1)}$, which are again indistinguishable. The relative error given by (50) is shown in Fig. 3(b), where we observe that it is $O(1)$.

Another interesting example is toothpaste. Table 2 shows typical values for toothpaste reported in [24]. We observe significant differences in the values of density, yield stress, and viscosity compared to those in Table 1.

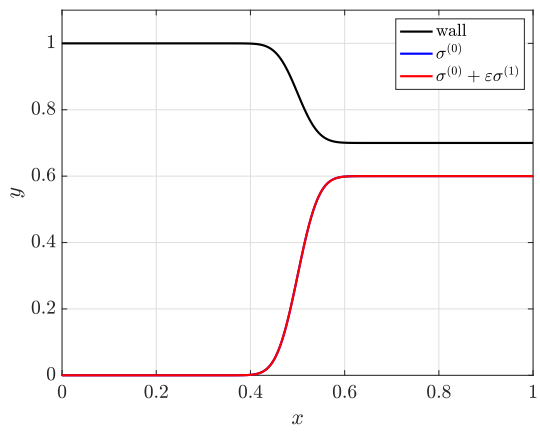
Fig. 4(a) shows the yield surfaces $\sigma^{(0)}$ and $\sigma^{(0)}+\varepsilon\sigma^{(1)}$. The relative error is shown in Fig. 4(b), where we see that it remains $O(1)$, though slightly smaller than in the case of drilling muds.

7. Conclusions

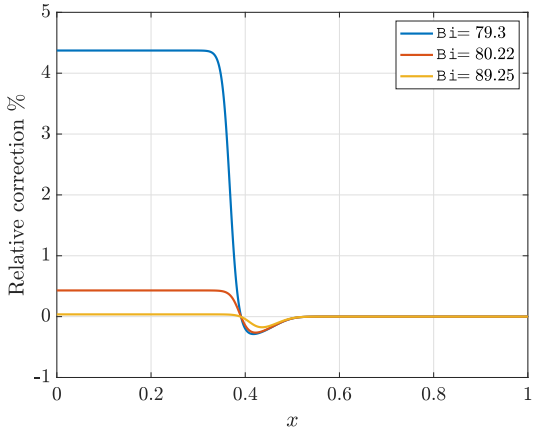
The present analysis assumes a sharp yield surface and a continuous rigid plug extending from inlet to outlet, with no wall slip and planar two-dimensional flow. If the leading-order yield surface $\sigma^{(0)}(x)$ vanishes locally, the integral momentum balance for the rigid core degenerates and the asymptotic structure breaks down, so that plug rupture or re-yielding cannot be captured within the present framework. Addressing such situations would require a different asymptotic scaling or a local analysis near the rupture points.

The integral momentum balance employed here differs fundamentally from pseudo-plug theory of [4] in that the inner core is treated as a rigid body with indeterminate internal stress, whose velocity is determined by a global force balance rather than by weak yielding. The first-order analysis provides explicit analytical expressions for corrections to the velocity field, pressure gradient, and yield surface, allowing a quantitative assessment of the accuracy of lubrication-type approximations. While no direct numerical comparison is performed, our results are consistent with the qualitative trends reported in [4] (see for instance the opposite monotonicity of the yield surface).

The present sharp-interface formulation differs also from regularized constitutive models (e.g., Papanastasiou or bi-viscosity models), which smooth the yield transition. While regularized models avoid stress discontinuities, the sharp-interface approach allows an exact enforcement of the yield condition and avoids the introduction of additional regularization parameters. We remark that in our approach the stress field is not required to be fully determined inside the rigid

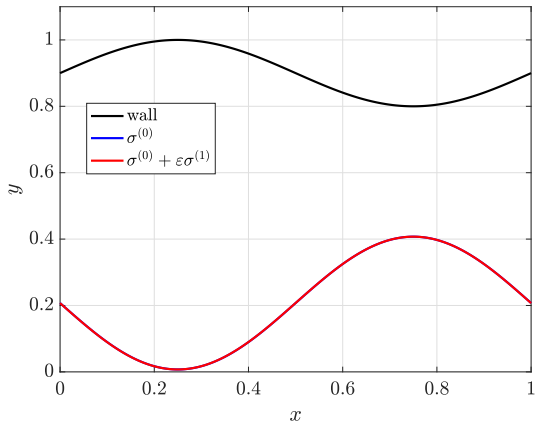


(a) Channel wall and yield surface with $h(x)$ as in (49)

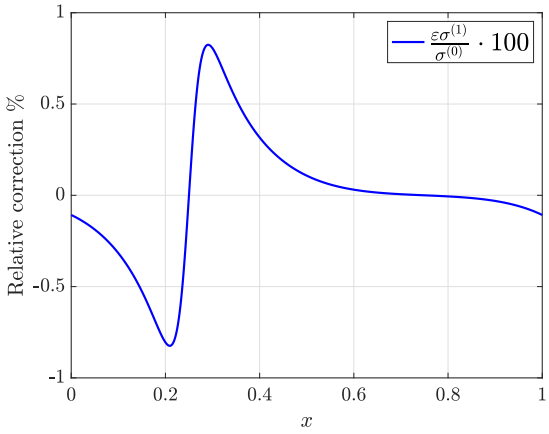


(b) Relative error (50) for Bi = 79.30, 80.22, 89.25.

Fig. 2. (a) Channel wall and yield surface at zero and first order for $h(x)$ as in (49); (b) relative error (50).

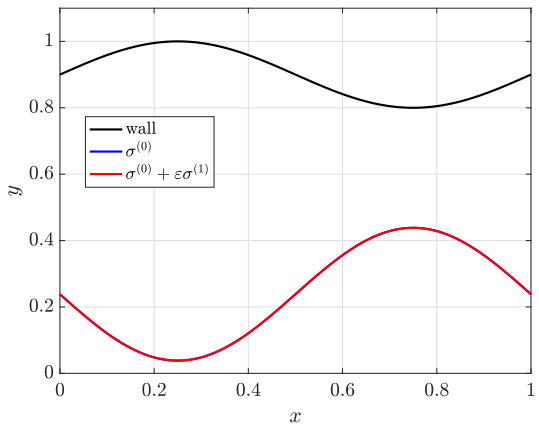


(a) Channel wall and yield surface with $h(x)$ as in (51)

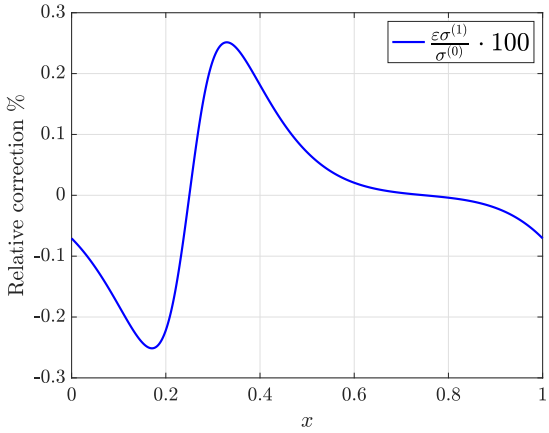


(b) Relative error (50) for Bi = 2.5.

Fig. 3. (a) Channel wall and yield surface at zero and first order for $h(x)$ as in (51).



(a) Channel wall and yield surface with $h(x)$ as in (51)



(b) Relative error (50) for Bi = 3.12.

Fig. 4. (a) Channel wall and yield surface at zero and first order for $h(x)$ as in (51).

core, and that the integral momentum balance avoids the need to resolve possible stress singularities near yield-surface endpoints.

The numerical examples provided are intended to be illustrative rather than exhaustive. They quantify the magnitude of first-order corrections within the asymptotic regime of validity and do not constitute a full validation against DNS or experimental data. The reported $O(10\%)$ corrections occur only for specific combinations of geometry and rheological parameters, and no claim of generality is implied.

The asymptotic strategy developed here for planar channels can, in principle, be extended to axisymmetric tubes with slowly varying radius (see [25]), along the lines of previous zero-order analyses. Such an extension would require accounting for curvature effects in the momentum balance of the rigid core, but the linear structure of the higher-order problems is expected to be preserved.

The main assumptions and limitations of the model considered in this study can be summarized as follows: (i) sharp-interface assumption; (ii) no-slip boundary conditions; (iii) planar geometry; (iv) steady-state two-dimensional flow. Any extension of these assumptions will certainly modify the shape of the inner core.

We analyzed the steady flow of a Bingham fluid in a channel with non-flat walls by developing an asymptotic expansion in the geometric aspect ratio ε. The leading-order solution recovers the classical structure with a continuous rigid core, determined through a nonlinear algebraic equation ensuring existence and uniqueness under appropriate geometric and rheological conditions. The first-order analysis shows that all corrections can be expressed in terms of the correction to the rigid-core velocity, which acts as the key parameter of the higher-order problems. A noteworthy outcome is that, although not rigorously proven, the equations at order one (and likewise at all higher orders) are linear in the unknowns and involve coefficients that remain bounded, since they depend solely on the zero-order solution. As a consequence, first-order corrections, and thus all higher-order ones, remain bounded in an appropriate norm, ensuring that the remainder of the expansion stays controlled for every truncation order. This structural property indicates that the full asymptotic expansion is formally well-posed at all orders.

Finally, numerical examples confirm that first-order terms are typically negligible, except in specific parameter ranges where they may reach up to 10% of the leading-order contributions, thereby clarifying both the robustness and the applicability limits of the resulting approximation.

CRediT authorship contribution statement

Lorenzo Fusi: Writing – review & editing, Writing – original draft, Methodology, Investigation, Conceptualization. **Angiolo Farina:** Writing – review & editing, Writing – original draft, Methodology, Investigation, Conceptualization.

Declaration of competing interest

The authors declare that they have no known competing financial interests or personal relationships that could have appeared to influence the work reported in this paper.

Acknowledgments

The present work has been carried out under the auspices of the Italian National Group for Mathematical Physics (GNFM-Indam). This work has been performed within the PRIN 2022 project “Mathematical modelling of heterogeneous systems”, financed by the European Union - Next Generation EU, CUP B53D23009360006/B53D23009370006, Project Code 2022MKB7MM, PNRR M4.C2.1.1.

Data availability

No data was used for the research described in the article.

References

[1] R.R. Huilgol, Fluid Mechanics of Viscoplasticity, Springer, 2015.
[2] J.G. Oldroyd, A rational formulation of the equations of plastic flow for a Bingham solid, in: Mathematical Proceedings of the Cambridge Philosophical Society, Vol. 43, Cambridge University Press, 1947, pp. 100–105.
[3] K.v. Hohenemser, W. Prager, Über die ansätze der mechanik isotroper kontinua, ZAMM-Journal Appl. Math. Mech./Z. Angew. Math. Mech. 12 (4) (1932) 216–226.
[4] I. Frigaard, D. Ryan, Flow of a visco-plastic fluid in a channel of slowly varying width, J. Non-Newton. Fluid Mech. 123 (1) (2004) 67–83.
[5] A. Putz, I. Frigaard, D. Martinez, On the lubrication paradox and the use of regularisation methods for lubrication flows, J. Non-Newton. Fluid Mech. 163 (1–3) (2009) 62–77.
[6] N. Balmforth, R. Craster, A consistent thin-layer theory for Bingham plastics, J. Non-Newton. Fluid Mech. 84 (1) (1999) 65–81.
[7] M. Philippou, Z. Kountouriotis, G.C. Georgiou, Viscoplastic flow development in tubes and channels with wall slip, J. Non-Newton. Fluid Mech. 234 (2016) 69–81.
[8] L. Muravleva, Axisymmetric squeeze flow of a viscoplastic Bingham medium, J. Non-Newton. Fluid Mech. 249 (2017) 97–120.
[9] P. Panaseti, G.C. Georgiou, Viscoplastic flow development in a channel with slip along one wall, J. Non-Newton. Fluid Mech. 248 (2017) 8–22.
[10] K.D. Housiadas, I. Ioannou, G.C. Georgiou, Lubrication solution of the axisymmetric poiseuille flow of a Bingham fluid with pressure-dependent rheological parameters, J. Non-Newton. Fluid Mech. 260 (2018) 76–86.
[11] C. Dorier, J. Tichy, Behavior of a Bingham-like viscous fluid in lubrication flows, J. Non-Newton. Fluid Mech. 45 (3) (1992) 291–310.
[12] S.G. Lampaert, R.A. van Ostayen, Lubrication theory for Bingham plastics, Tribol. Int. 147 (2020) 106160.
[13] I. Frigaard, Simple yield stress fluids, Curr. Opin. Colloid Interface Sci. 43 (2019) 80–93.
[14] P. Coussot, Yield stress fluid flows: A review of experimental data, J. Non-Newton. Fluid Mech. 211 (2014) 31–49.
[15] N.J. Balmforth, I.A. Frigaard, G. Ovarlez, Yielding to stress: recent developments in viscoplastic fluid mechanics, Annu. Rev. Fluid Mech. 46 (1) (2014) 121–146.
[16] G. Lipscomb, M. Denn, Flow of Bingham fluids in complex geometries, J. Non-Newton. Fluid Mech. 14 (1984) 337–346.
[17] I. Walton, S. Bittleston, The axial flow of a Bingham plastic in a narrow eccentric annulus, J. Fluid Mech. 222 (1991) 39–60.
[18] A. Farina, L. Fusi, Viscoplastic fluids: Mathematical modeling and applications, in: Non-Newtonian Fluid Mechanics and Complex Flows: Levico Terme, Italy 2016, Springer, 2018, pp. 229–298.
[19] L. Fusi, A. Farina, F. Rosso, On the mathematical paradoxes for the flow of a viscoplastic film down an inclined surface, Int. J. Non-Linear Mech. 58 (2014) 139–150.
[20] L. Fusi, A. Farina, F. Rosso, S. Roscani, Pressure driven lubrication flow of a Bingham fluid in a channel: A novel approach, J. Non-Newton. Fluid Mech. 221 (2015) 66–75.
[21] A. Farina, L. Fusi, L. Vergori, E. Zanetti, Viscoplastic flows in channels with small aspect ratio: Bingham versus regularised models, Internat. J. Engrg. Sci. 199 (2024) 104074.
[22] P. Panaseti, Y. Damianou, G.C. Georgiou, K.D. Housiadas, Pressure-driven flow of a Herschel-Bulkley fluid with pressure-dependent rheological parameters, Phys. Fluids 30 (3) (2018).
[23] R.P. Chhabra, S.A. Patel, Non-Newtonian Flow and Applied Rheology: Engineering Applications, Elsevier, 2025.
[24] A. Ahuja, A. Potanin, Rheological and sensory properties of toothpastes, Rheol. Acta 57 (6) (2018) 459–471.
[25] L. Fusi, K.D. Housiadas, G.C. Georgiou, Flow of a Bingham fluid in a pipe of variable radius, J. Non-Newton. Fluid Mech. 285 (2020) 104393.